20. M. W. Bevan, M. D. Chilton, *Annu. Rev. Genet.* **16**, 357–384 (1982).
21. Y. Ding, Y. Fu, J. C. Lee, D. C. Hooper, *J. Bacteriol.* **194**, 6586–6593 (2012).
22. Materials and methods are available as supplementary materials on *Science* Online.
23. J. Thompson, J. A. Donkersloot, *Annu. Rev. Biochem.* **61**, 517–554 (1992).
24. P. T. Chivers, E. L. Benanti, V. Heil-Chapdelaine, J. S. Iwig, J. L. Rowe, *Metallomics* **4**, 1043–1050 (2012).
25. H. Lebrette, M. Iannello, J. C. Fontecilla-Camps, C. Cavazza, *J. Inorg. Biochem.* **121**, 16–18 (2013).
26. M. M. Shaik, L. Cendron, M. Salamina, M. Ruzzene, G. Zanotti, *Mol. Microbiol.* **91**, 724–735 (2014).
27. W. Vollmer, D. Blanot, M. A. de Pedro, *FEMS Microbiol. Rev.* **32**, 149–167 (2008).
28. F. Cava, M. A. de Pedro, H. Lam, B. M. Davis, M. K. Waldor, *EMBO J.* **30**, 3442–3453 (2011).
29. H. Lam *et al.*, *Science* **325**, 1552–1555 (2009).
30. I. Kolodkin-Gal *et al.*, *Science* **328**, 627–629 (2010).
31. A. T. Anfora, B. J. Haugen, P. Roesch, P. Redford, R. A. Welch, *Infect. Immun.* **75**, 5298–5304 (2007).
32. K. A. O'Connor, D. R. Zusman, *Mol. Microbiol.* **24**, 839–850 (1997).
33. M. Gi *et al.*, *Sci. Rep.* **5**, 14644 (2015).

ACKNOWLEDGMENTS

We thank the Commissariat à l'Energie Atomique et aux Energies Alternatives (CEA), the Agence Nationale de la Recherche (ANR, program ANR-14-CE09-0007), and the CEA program ToxNuc-E for financial support. Support was also provided by the HélioBiotec platform (funded by the European Regional Development Fund, the Région Provence Alpes Côte d'Azur, the French Ministry of Research, and the "Commissariat à l'Energie Atomique et aux Energies Alternatives"). G.G. was supported by the Région PACA. Work at the F.C. lab was supported by the Laboratory for Molecular Infection Medicine Sweden, the Knut and Alice Wallenberg Foundation, the Swedish Research Council, and a Kempe foundation scholarship to A.E. S.W. was supported by a fellowship from the Chinese Scholarship Council. We thank J. Lavergne for careful reading of the manuscript and A. Verméglio, C. Cavazza, and H. Lebrette for fruitful discussions. All data are presented in the supplementary materials.

SUPPLEMENTARY MATERIALS

www.sciencemag.org/content/352/6289/1105/suppl/DC1
Materials and Methods
Figs. S1 to S16
Tables S1 to S3
References (*34*–*49*)

17 December 2015; accepted 12 April 2016
10.1126/science.aaf1018

ATMOSPHERIC PARTICLES

New particle formation in the free troposphere: A question of chemistry and timing

F. Bianchi,[1,2,3]* J. Tröstl,[1] H. Junninen,[3] C. Frege,[1] S. Henne,[4] C. R. Hoyle,[1,5] U. Molteni,[1] E. Herrmann,[1] A. Adamov,[3] N. Bukowiecki,[1] X. Chen,[3] J. Duplissy,[3,6] M. Gysel,[1] M. Hutterli,[7] J. Kangasluoma,[3] J. Kontkanen,[3] A. Kürten,[8] H. E. Manninen,[3] S. Münch,[8] O. Peräkylä,[3] T. Petäjä,[3] L. Rondo,[8] C. Williamson,[8]† E. Weingartner,[1]‡ J. Curtius,[8] D. R. Worsnop,[3,9] M. Kulmala,[3] J. Dommen,[1] U. Baltensperger[1]*

New particle formation (NPF) is the source of over half of the atmosphere's cloud condensation nuclei, thus influencing cloud properties and Earth's energy balance. Unlike in the planetary boundary layer, few observations of NPF in the free troposphere exist. We provide observational evidence that at high altitudes, NPF occurs mainly through condensation of highly oxygenated molecules (HOMs), in addition to taking place through sulfuric acid–ammonia nucleation. Neutral nucleation is more than 10 times faster than ion-induced nucleation, and growth rates are size-dependent. NPF is restricted to a time window of 1 to 2 days after contact of the air masses with the planetary boundary layer; this is related to the time needed for oxidation of organic compounds to form HOMs. These findings require improved NPF parameterization in atmospheric models.

Atmospheric aerosols influence climate through direct interaction with radiation and by acting as cloud condensation nuclei (*1*, *2*). There is considerable uncertainty about what fraction of cloud condensation nuclei is attributable to new particle formation (NPF) (*3*–*5*). Studies of NPF in the free troposphere have used ground-based (*6*–*9*) and airborne (*10*) platforms but with limited instrumentation and/or over short time scales. Because of the lack of data at high altitudes, the vast majority of models use free-troposphere NPF schemes in which particle formation rates depend only on the concentration of sulfuric acid, relative humidity, and temperature (*11*). Recently, comprehensive NPF measurements performed as part of the CLOUD (Cosmics Leaving Outdoor Droplets) project detected ternary nucleation of sulfuric acid with water and oxidized organics (*12*). Implementation of this NPF scheme in GLOMAP (Global Model of Aerosol Processes) (*13*) yielded a photochemically and biologically driven seasonal cycle of particle concentrations in the continental boundary layer, comparable to observations (*12*). Further CLOUD experiments observed NPF without involvement of sulfuric acid, which is expected to be important especially in pristine regions and the preindustrial atmosphere (*14*). These laboratory and modeling studies call for field verification.

To chemically and physically characterize the early stage of NPF in the free troposphere, we used a suite of state-of-the-art mass spectrometers and particle counters at the high-altitude research station Jungfraujoch (JFJ), Switzerland [3580 m above sea level (*15*)]. At this site, NPF occurs on 15 to 20% of days, without apparent seasonal dependence (fig. S9), as shown by long-term observations (*16*) and dedicated campaigns (*17*). We report measurements collected over the period of a year, including two intensive 1-month campaigns (table S1).

We identified three typical situations, represented by consecutive example days (days 1 to 3) (Fig. 1); in addition, we show a special case (day 4) where the sulfuric acid concentration was unusually high (~6×10^6 cm^{-3}). Day 1 (25 February 2014) is an example of one of the many non-event days during sunny conditions. During the afternoon, there is a slight enhancement in the concentration of 5- to 10-nm particles, but the simultaneous increase in larger particles (up to 90 nm) suggests that this enhancement is related to vertical transport of particles formed elsewhere (*15*). Day 2 (26 February 2014) is typical of days when the JFJ is within clouds, when NPF is suppressed by reduced global radiation and the high condensation sink of the cloud droplets. Days 3 and 4 (27 February and 2 March 2014) are two examples of NPF days, classified as 1A events (*15*), where the number concentration of particles larger than 3.2 nm increases strongly from a few hundred to 40,000 cm^{-3}.

On most sunny days, the sulfuric acid concentration followed a consistent diurnal cycle, with concentrations <10^4 cm^{-3} during the night and ≤5×10^5 cm^{-3} during the day (except day 4, which had much higher concentrations). However, no link was found between sulfuric acid and NPF, suggesting that sulfuric acid at these concentrations does not explain NPF at the JFJ (Fig. 1D). Highly oxygenated molecules (HOMs), which we detected with a chemical ionization–atmospheric pressure interface–time of flight mass spectrometer (CI-APi-TOF), were formed on some sunny days (e.g., day 3) but not on others (e.g., day 1) (Fig. 1D). This variability is probably dependent on the presence of organic precursors in the free troposphere. Figure 1E shows the time evolution

[1]Laboratory of Atmospheric Chemistry, Paul Scherrer Institute, 5232 Villigen, Switzerland. [2]Institute for Atmospheric and Climate Science, ETH Zurich, 8092 Zurich, Switzerland. [3]Department of Physics, University of Helsinki, 00014 Helsinki, Finland. [4]Empa, Swiss Federal Laboratories for Materials Science and Technology, 8600 Dübendorf, Switzerland. [5]WSL (Swiss Federal Institute for Forest, Snow and Landscape Research) Institute for Snow and Avalanche Research SLF, 7260 Davos, Switzerland. [6]Helsinki Institute of Physics, University of Helsinki, 00014 Helsinki, Finland. [7]Tofwerk, 3600 Thun, Switzerland. [8]Institute for Atmospheric and Environmental Sciences, Goethe University Frankfurt, 60438 Frankfurt am Main, Germany. [9]Aerodyne Research, Billerica, MA 01821, USA.
***Corresponding author. Email: federico.bianchi@psi.ch (F.B.); urs.baltensperger@psi.ch (U.B.)** †Present address: Cooperative Institute for Research in Environmental Sciences, University of Colorado, Boulder, CO 80309, USA. ‡Present address: Institute for Aerosol and Sensor Technology, University of Applied Sciences (FHNW), 5210 Windisch, Switzerland.

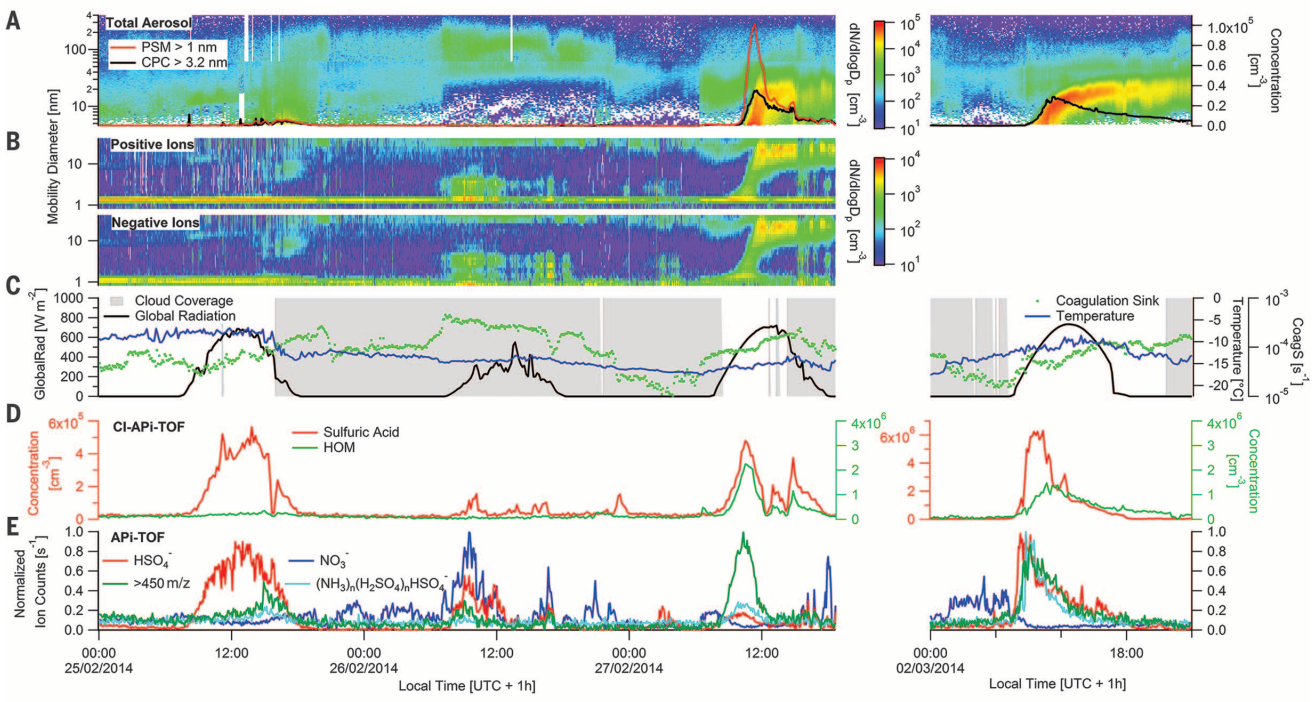

Fig. 1. Four representative situations observed at the JFJ. Shown are data from a sunny day with no nucleation (25 February, day 1), a cloudy day (26 February, day 2), a nucleation day with HOMs (27 February, day 3); and a nucleation day with H_2SO_4, NH_3, and HOMs (2 March, day 4) (h, hours). (**A**) Particle size distribution ($dN/d\log D_p$), measured with a nano-SMPS (scanning mobility particle sizer), and particle number concentration above 1 and 3.2 nm, measured with a particle size magnifier (PSM) and a condensation particle counter (CPC), respectively. (**B**) Size distributions of the positive and negative ions measured by the NAIS. (**C**) Global radiation, temperature, coagulation sink, and cloud coverage. (**D**) Concentrations of sulfuric acid (red) and HOMs (green) measured with the CI-APi-TOF. A different axis is used for sulfuric acid in the right panel. (**E**) Measurements of specific ions with the APi-TOF (HSO_4^- in red, NO_3^- in blue, and the sum of ions with m/z >400 Th in green). The clusters containing sulfuric acid and ammonia are shown by the light blue line.

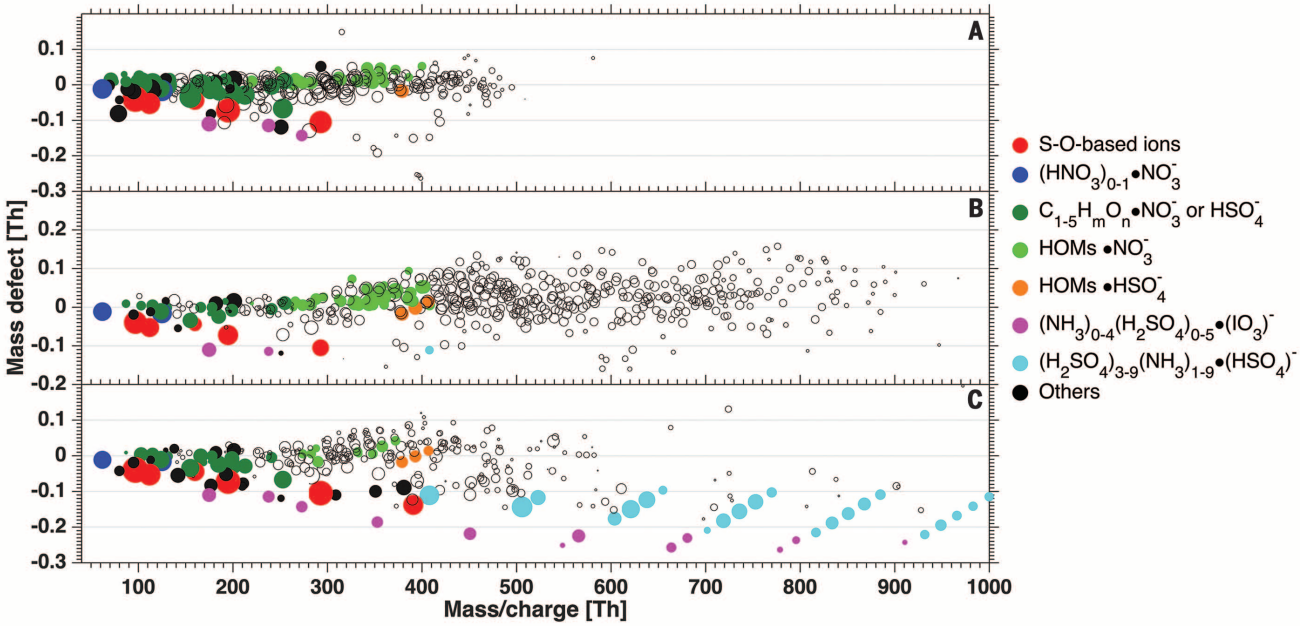

Fig. 2. Mass defect plots (negative ions). (**A**) Measurements from day 1, (**B**) day 3, and (**C**) day 4. The abscissa shows the mass/charge ratio and the ordinate shows the mass defect, which is the difference between the nominal (integer) mass and the exact mass. Colors relate to pure sulfuric acid clusters (red), nitrate (blue), small organic compounds alone or clustered with NO_3^- or HSO_4^- (dark green), HOMs clustered with NO_3^- (light green), HOMs clustered with HSO_4^- (orange), H_2SO_4-NH_3-HIO_3 (violet), and H_2SO_4-NH_3 clusters (light blue). Open circles represent unidentified peaks. The marker size is proportional to the logarithm of the count rate. The mass spectra for the same events are shown in fig. S3.

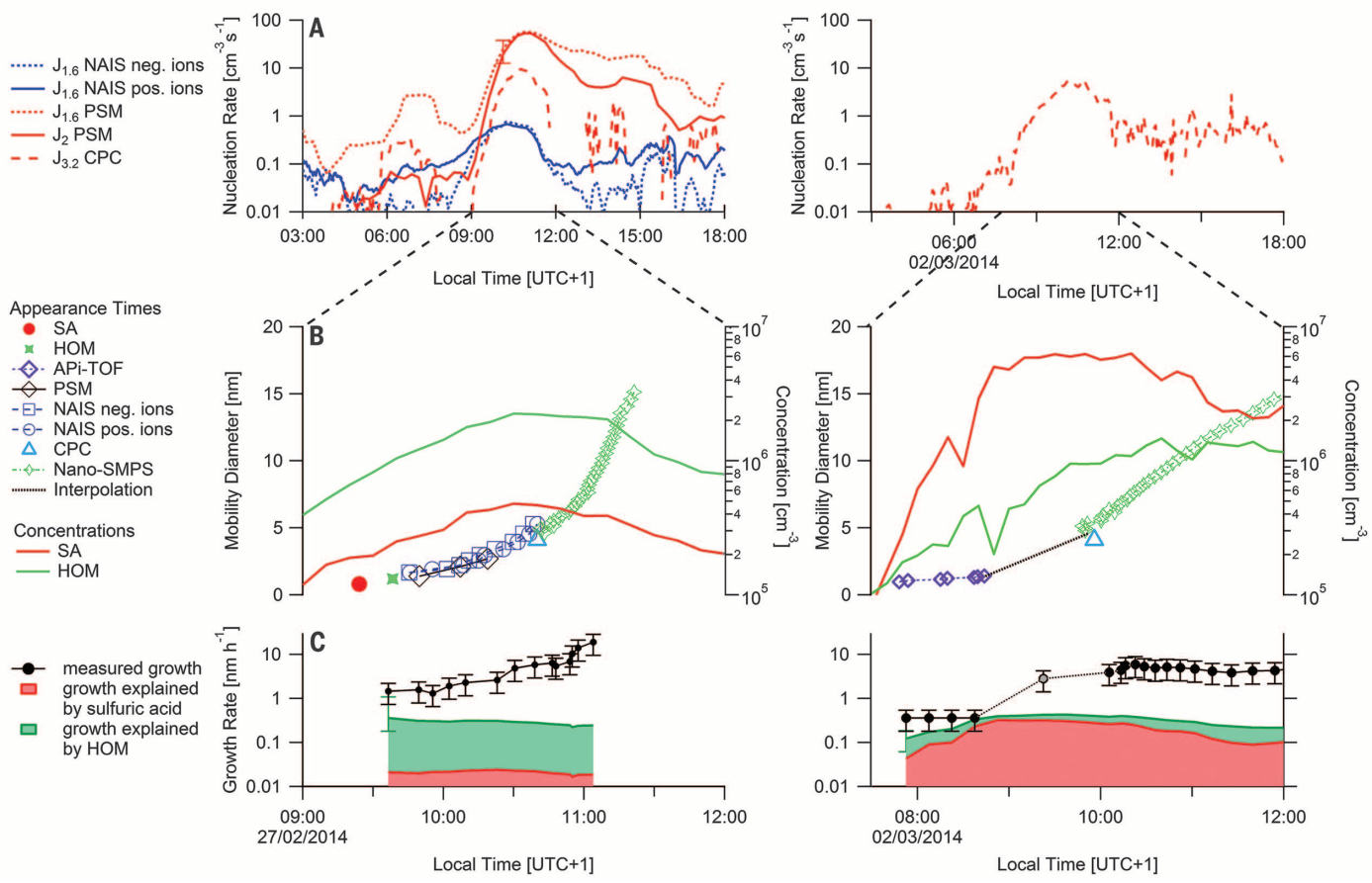

Fig. 3. Particle evolution during the nucleation events observed on days 3 and 4. Throughout, data for day 3 are shown on the left, and data from day 4 are shown on the right. (**A**) Formation rates (J) of the particles and ions at different sizes. (**B**) Evolution of particle diameter during the nucleation events. The two solid lines (red and green) show the concentrations of sulfuric acid (SA) and HOMs. (**C**) Comparison of the measured growth rates (black; error bars indicate systematic scale uncertainty) with growth rates calculated by assuming that solely sulfuric acid contributes to the growth (red) (*30*) or by also assuming a contribution from HOMs (green) (*29*). In addition to a much higher sulfuric acid concentration, the data for day 4 show a $J_{3.2}$ and growth rate that are slightly lower than those of day 3. On day 4, not all of the instruments required to measure particles across the full range from 1 to 15 nm were functioning. Therefore, the growth rate was interpolated between about 08:40 and 10:00.

of several negative ions measured with an APi-TOF: HSO_4^-, NO_3^-, the family of clusters containing NH_3 and H_2SO_4, and ions with mass/charge ratios m/z > 400 thomsons (Th; 1 Th = 1 Da e^{-1}, where e is the elementary charge), which are likely to be mainly organic compounds (*15*). Nucleation nearly exclusively occurred on days when the concentration of organic compounds was high. The nucleation event on day 4 had a somewhat different ion cluster composition; the organic ions were present, but HSO_4^- and the H_2SO_4-NH_3 cluster family were of equal magnitude, probably because the H_2SO_4 concentration was very high (Fig. 1). However, throughout the year of APi-TOF measurements, we never observed pure H_2SO_4 clusters with more than four molecules (table S3), confirming the findings of previous studies, which showed that binary H_2SO_4-H_2O nucleation does not explain atmospheric NPF (*18*, *19*).

The role of HOMs is further illustrated in Fig. 2, which shows mass defect plots (*20*, *21*) for negative ions for three of the days depicted in Fig. 1 (fig. S4 shows plots for corresponding neutral clusters). During the sunny day without NPF (day 1), most of the ions observed had m/z values <300 Th and were small acid clusters. These ions appear to be spectators (ions that are always present but unlikely to participate in cluster growth, such as nitrate, oxalate, and other organic acids that are too volatile to condense on such small particles). The smaller ions observed on day 3 (Fig. 2B) did not greatly differ from those observed on day 1; however, many ions with m/z values >300 Th were also present. The organic contribution is confirmed by the chemical composition of neutral clusters, shown in figs. S4 and S5 and table S2. The most intense organic peaks measured by the APi-TOF overlap with those measured by the CI-APi-TOF. In both cases, we attribute these peaks to HOMs clustered with nitrate (table S2). The difference is that in one case (in which ions were detected by the APi-TOF), the HOMs were clustered with NO_3^- in the ambient atmosphere, whereas neutral HOMs were clustered with NO_3^- inside the CI-APi-TOF ion source. Even though the chemical formulae of these HOMs differ from those of HOMs generated by monoterpene oxidation (*22*–*25*), they are similar in mass range and O:C ratio. They are therefore expected to have similarly low volatility and nucleating properties. Chemical identification of the negative ions detected on day 3 (Fig. 2 and fig. S5) indicates that the HOMs cluster exclusively with NO_3^-, except the three most abundant peaks, which also cluster to a minor extent with HSO_4^- (peaks 2a, 3a, and 4a in fig. S5). This confirms recent CLOUD findings that sulfuric acid is not important for NPF (*14*) at this concentration.

On day 4, we detected a distinctive sequence of ions, $(H_2SO_4)_m(NH_3)_nHSO_4^-$ (where m and n are integers varying from 3 to 9 and from 1 to 9, respectively), which closely resembles the sequence identified in CLOUD experiments involving purely H_2SO_4-NH_3 nucleation (*18*, *20*, *21*). In addition to this sequence, we observed other similar clusters in which the charging ion was IO_3^- instead of HSO_4^- (pink dots, Fig. 2). However, because these ions were only a minor fraction of all the clusters, and only a single iodate was found, we do not consider iodate to be important for this nucleation event.

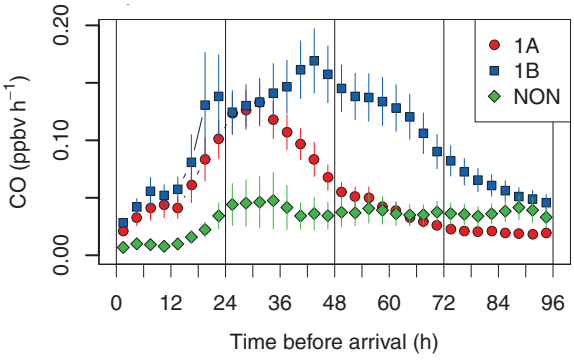

Fig. 4. Uptake of anthropogenic carbon monoxide versus time before arrival at the JFJ, for air masses sampled under different nucleation conditions. Shown are simulated means (symbols) and standard uncertainties of the means (error bars). Type 1A events (red) include pronounced and clearly identifiable events, type 1B events (blue) include less well-defined nucleation events, and NON (green) indicates no nucleation events.

On day 3, the total particle formation rate J decreased as a result of the coagulation processes that occur with increasing size, with $J_{1.6}$ = 51 cm^{-3} s^{-1} and J_2 = 46 cm^{-3} s^{-1} (where subscripts denote mobility diameter in nanometers) (Fig. 3A). The formation rates of positive and negative ions with a diameter of 1.6 nm, determined from neutral cluster air ion spectrometer (NAIS) ion-mode measurements, were much lower (<1 cm^{-3} s^{-1}) than those of the neutral particles of the same size, suggesting that the neutral process dominated (*26*) in this nucleation event. CLOUD results for pure sulfuric acid nucleation indicate a $J_{1.7}$ below 10^{-5} cm^{-3} s^{-1} (*27*) at a similar concentration and temperature. There is strong indication of the presence of HOMs in the nucleating clusters but not of ammonia or amines. Because the saturation concentration is expected to decrease substantially with decreasing temperature, we consider this to be in good agreement with the findings of Kirkby *et al.* (*14*), who reported $J_{1.7}$ = 40 cm^{-3} s^{-1} at [HOM] = 4 × 10^8 cm^{-3} and temperature T = 5°C.

On day 4, the observed $J_{3.2}$ of ~4.5 cm^{-3} s^{-1} at temperatures between −12°C and −15°C was similar to that measured by CLOUD: $J_{1.7}$ ~ 4 cm^{-3} s^{-1} for [H_2SO_4] = 6 × 10^6 cm^{-3} and [NH_3] = 1 part per billion by volume (ppbv) at T = −15°C (*18*). Because the ammonia concentration during this event at the JFJ is expected to have been lower than 1 ppbv, we hypothesize a synergistic effect of H_2SO_4, NH_3, and nonnegligible concentrations of HOMs. This event was a special case where the sulfuric acid concentration was extremely high. However, APi-TOF measurements show that HOMs were present in the initial clusters in 13 out of 19 nucleation events (type 1A or 1B; table S3). Nucleation thus appears to be influenced by the presence of organic compounds in the majority of cases. The importance of HOMs is further illustrated by the size-dependent growth rates observed during particle formation (Fig. 3), confirming that nano-Köhler growth (*3*) also applies in free troposphere conditions. On day 3, the growth rate was initially driven by HOMs and continued to increase after the HOM concentration began to decline, probably due to a reduced Kelvin effect at larger particle sizes, enabling the condensation of more volatile (unmeasured) molecules (fig. S8) (*28*) [as recently found in laboratory experiments (*29*)]. On day 4, a greater part of the initial growth rate can be explained by sulfuric acid and water under the assumption of condensation at the kinetic limit (fig. S7) (*30*). After that, the higher growth rate cannot be explained by sulfuric acid alone, which is again probably indicative of condensation of more volatile (unmeasured) molecules (*29*) on the newly formed particles, showing that this process is also not entirely inorganic.

An important question is where the condensable vapors or their precursors originate. We used the Lagrangian particle dispersion model FLEXPART in time-inverse mode and compared air mass origins of all the major events (type 1A and 1B) with those of typical non-event days during the same period (*15*). Increases in simulated carbon monoxide concentration and the strength of the source-receptor relationship, indicative of influence by the planetary boundary layer, were evident in individual backward simulations (Fig. 4 and fig. S10). This suggests an anthropogenic source of the HOM precursors but does not preclude a biogenic source. For all simulated cases, the small increase in CO within 6 hours before air mass arrival suggests no substantive influence from local emissions during this period. Air masses experienced enhanced uptake of CO and also an increase in the strength of the source-receptor relationship (fig. S11) 12 to 40 hours before type 1A events were detected at the JFJ, caused by contact with polluted boundary layer air. Similarly, air masses connected to type 1B events experienced increased CO uptake, though somewhat farther upwind, between 12 and 72 hours before arrival at the JFJ, with a maximum uptake at 48 hours. In contrast, for non-event days, CO uptake was considerably below that during nucleation events. This indicates that one requirement for observing NPF at the JFJ is nonlocal contact (fig. S12) with the planetary boundary layer and, hence, the uptake of emissions hours before arrival at the JFJ, allowing a sufficiently long processing time in the free troposphere. An optimal transport time from the planetary boundary layer to foster nucleation appears to be around 1 day, whereas longer transport times result in less clear nucleation events, due to ongoing oxidation and dilution of the precursor gases.

Combining in situ observations and modeling results, we thus find that NPF in the free troposphere depends on the availability of highly oxidized organic species, providing confirmation for NPF pathways observed in recent laboratory experiments. The availability of these highly oxidized organic species in turn depends on previous surface contact of the air mass and appropriate time to process the precursors from the boundary layer on their way up. In short, chemistry and timing play the main roles. To properly represent nucleation in the free troposphere, future atmospheric models should take these factors into account.

REFERENCES AND NOTES

1. T. L. Anderson *et al.*, *Bull. Am. Meteorol. Soc.* **86**, 1795–1809 (2005).
2. R. J. Charlson *et al.*, *Science* **255**, 423–430 (1992).
3. M. Kulmala *et al.*, *J. Aerosol Sci.* **35**, 143–176 (2004).
4. J. Merikanto, D. V. Spracklen, G. W. Mann, S. J. Pickering, K. S. Carslaw, *Atmos. Chem. Phys.* **9**, 8601–8616 (2009).
5. R. Zhang, A. Khalizov, L. Wang, M. Hu, W. Xu, *Chem. Rev.* **112**, 1957–2011 (2012).
6. S. Rodríguez *et al.*, *Atmos. Chem. Phys.* **9**, 6319–6335 (2009).
7. C. Rose *et al.*, *Atmos. Environ.* **102**, 18–29 (2015).
8. H. Venzac *et al.*, *Proc. Natl. Acad. Sci. U.S.A.* **105**, 15666–15671 (2008).
9. F. Q. Yu, A. G. Hallar, *J. Geophys. Res. Atmos.* **119**, 12246–12255 (2014).
10. S. Mirme *et al.*, *Atmos. Chem. Phys.* **10**, 437–451 (2010).
11. M. Kulmala, A. Laaksonen, L. Pirjola, *J. Geophys. Res. Atmos.* **103**, 8301–8307 (1998).
12. F. Riccobono *et al.*, *Science* **344**, 717–721 (2014).
13. G. W. Mann *et al.*, *Geosci. Model Dev.* **3**, 519–551 (2010).
14. J. Kirkby *et al.*, *Nature* 10.1038/nature17953 (2016).
15. Materials and methods are available as supplementary materials on *Science* Online.
16. E. Herrmann *et al.*, *J. Geophys. Res. Atmos.* **120**, 9459–9480 (2015).
17. J. Boulon *et al.*, *Atmos. Chem. Phys.* **10**, 9333–9349 (2010).
18. J. Kirkby *et al.*, *Nature* **476**, 429–433 (2011).
19. F. L. Eisele *et al.*, *J. Geophys. Res. Atmos.* **111**, D04305 (2006).
20. F. Bianchi *et al.*, *Environ. Sci. Technol.* **48**, 13675–13684 (2014).
21. S. Schobesberger *et al.*, *Proc. Natl. Acad. Sci. U.S.A.* **110**, 17223–17228 (2013).
22. M. Ehn *et al.*, *Nature* **506**, 476–479 (2014).
23. T. Jokinen *et al.*, *Proc. Natl. Acad. Sci. U.S.A.* **112**, 7123–7128 (2015).
24. T. F. Mentel *et al.*, *Atmos. Chem. Phys.* **15**, 6745–6765 (2015).
25. M. P. Rissanen *et al.*, *J. Am. Chem. Soc.* **136**, 15596–15606 (2014).
26. C. Rose *et al.*, *Atmos. Chem. Phys.* **15**, 3413–3428 (2015).
27. J. Duplissy *et al.*, *J. Geophys. Res. Atmos.* **121**, 1752–1775 (2016).
28. M. Kulmala *et al.*, *Science* **339**, 943–946 (2013).
29. J. Tröstl *et al.*, *Nature* 10.1038/nature18271 (2016).
30. T. Nieminen, K. E. J. Lehtinen, M. Kulmala, *Atmos. Chem. Phys.* **10**, 9773–9779 (2010).

ACKNOWLEDGMENTS

We thank the International Foundation High Altitude Research Stations Jungfraujoch and Gornergrat for the opportunity to perform experiments at the Jungfraujoch and especially the research station's custodians J. and M. Fischer and M. and U. Otz for their support and hospitality. This work was supported by the Swiss National Science Foundation (grant nos. 200020_135307, 20020_152907, 206021_144947, and 200021_140663), MeteoSwiss in the framework of the Global Atmosphere Watch program, and the EC FP7 (European Commission Seventh Framework Programme for Research and Technological Development) project ACTRIS (Aerosols, Clouds, and Trace Gases Research Infrastructure Network) (grant agreement no. 262254). Funding was also received from the Academy of Finland Centre of Excellence (grant nos. 272041 and 1118615), the EC FP7 Marie Curie Initial Training Network (CLOUD-TRAIN, grant no. 316662), the German Federal Ministry of Education and Research (project no. 01LK1222A), the EC FP7 project BACCHUS (Impact of Biogenic Versus Anthropogenic Emissions on Clouds and Climate: Towards a Holistic Understanding; grant agreement no. 603445), and the European Research Council (grant no. 615922-BLACARAT). We thank the tofTools team for providing tools for mass spectrometry analysis. The authors declare no competing financial interests.

SUPPLEMENTARY MATERIALS

www.sciencemag.org/content/352/6289/1109/suppl/DC1
Materials and Methods
Figs. S1 to S12
Tables S1 to S4
References (*31*–*58*)

4 October 2015; accepted 29 March 2016
Published online 25 May 2016
10.1126/science.aad5456

New particle formation in the free troposphere: A question of chemistry and timing

F. Bianchi, J. Tröstl, H. Junninen, C. Frege, S. Henne, C. R. Hoyle, U. Molteni, E. Herrmann, A. Adamov, N. Bukowiecki, X. Chen, J. Duplissy, M. Gysel, M. Hutterli, J. Kangasluoma, J. Kontkanen, A. Kürten, H. E. Manninen, S. Münch, O. Peräkylä, T. Petäjä, L. Rondo, C. Williamson, E. Weingartner, J. Curtius, D. R. Worsnop, M. Kulmala, J. Dommen and U. Baltensperger (May 25, 2016)
Science **352** (6289), 1109-1112. [doi: 10.1126/science.aad5456]
originally published online May 25, 2016

Editor's Summary

From neutral to new

Many of the particles in the troposphere are formed in situ, but what fraction of all tropospheric particles do they constitute and how exactly are they made? Bianchi *et al.* report results from a high-altitude research station. Roughly half of the particles were newly formed by the condensation of highly oxygenated multifunctional compounds. A combination of laboratory results, field measurements, and model calculations revealed that neutral nucleation is more than 10 times faster than ion-induced nucleation, that particle growth rates are size-dependent, and that new particle formation occurs during a limited time window.

Science, this issue p. 1109

Science (print ISSN 0036-8075; online ISSN 1095-9203) is published weekly, except the last week in December, by the American Association for the Advancement of Science, 1200 New York Avenue NW, Washington, DC 20005.